

International Journal of Current Bio-Medical Engineering (IJCBE) Volume 1, Issue 2, November – December (2023)

RESEARCH ARTICLE

# TOUR-STAR: TUBERCULOSIS DETECTION USING DEEP LEARNING BASED SPIKING DILATED CONVOLUTIONAL NEURAL NETWORK

R. Shobana <sup>1,\*</sup>, Abitha V K Lija <sup>2</sup> and S. Shikky Marice <sup>3</sup>

<sup>1</sup> Assistant Professor, Department of Computer Science and Engineering, S.A. Engineering college, Chennai, Thiruverkadu, Tamil Nadu 600077 India.

<sup>2</sup> Assistant Professor, Department of Computer Science and Engineering, Meenakshi College of Engineering, Chennai, Tamil Nadu 600078 India.

\*Corresponding e-mail: rubanshobana@gmail.com

Abstract - Tuberculosis (TB) is among the most common communicable diseases caused by a bacterial infection namely Mycobacterium tuberculosis. The radiologists spend more time for detecting the TB when analysing with traditional methods. However, manual detection of TB is time-consuming and challenging task in the current scenario. To overcome these challenges, a novel deep learning-based TOUR-STAR model has been proposed for classifying the TB into three classes. Initially, the chest x-ray (CXR) images are gathered from the Pad Chest dataset and the collected images are pre-processed by Gaussian filter for reducing the noises and smoothen the edges. The Dual Attention U-Network is used to segment the liver region separately from the pre-processed CXR images. Finally, the segmented images are fed into spiking dilated convolutional neural network (SDCNN) to classify the TB into tri classes such as normal controls (NC), Pulmonary Tuberculosis (PT) and Miliary Tuberculosis (MT). The proposed TOUR-STAR model is evaluated based on its f1 score, precision, specificity, recall and accuracy. The classification accuracy of 98.90% for the proposed SDCNN are highly reliable for Pad Chest dataset. The proposed SDCNN outperforms ResNet, AlexNet, RegNet, and GoogleNet by 5.30%, 1.63%, 4.49% and 0.83% in terms of overall accuracy range. The suggested TOUR-STAR model achieves the overall accuracy by 0.20%, 0.76% and 4.14% comparing to the existing method such as CNN, DNN and EfficientNet.

**Keywords** – Tuberculosis, Chest X-ray image, Gaussian filter, Dual Attention U-Network, dilated attention convolutional neural network.

# 1. INTRODUCTION

Tuberculosis (TB) is a disease produced by mycobacterium that is transmissible. Humans are predominantly affected by pulmonary TB, but can also be affected by other parts of the body [1]. Every year, a large

number of TB patients die as a result of incorrect diagnoses, delayed diagnoses, and inadequate treatment [2]. The bacteria that cause tuberculosis is called Mycobacterium tuberculosis. Water, spitting, sneezing, and coughing are all ways for it to spread through the air. In addition to attacking the lungs (pulmonary TB), TBs often affects other organs, including the spine and bones (extrapulmonary TB) [3]. According to a WHO report, tuberculosis is the tenth largest cause of death and the second most prevalent transferable illness after COVID-19 [4]. CXR image screening is the greatest straightforward and widely used method of detecting TB in the lungs. A physician examination of chest radiographs is an additional option, although it is a time-consuming clinical process [5].

Recently, image classification techniques have been employed extensively to process and analyse images indepth using computer techniques, yielding positive classification and prediction findings [6]. Using chest radiological images, deep learning (DL) techniques have been functional with growing effectiveness to the quick, precise, and automated identification of lung diseases. For this reason, CXR is a low-priced, easily accessible, low-radiation-dose imagery method that is better than CT scans and MRI [7]. The key contributions of this work are summarized as,

- The primary purpose of this research is to designed a novel deep learning-based TOUR-STAR has been proposed for classifying the TB into three classes.
- Initially, the CXR images are gathered from the Pad Chest dataset and the collected images are

<sup>&</sup>lt;sup>3</sup> Research Scholar, Sri Krishna College of Engineering and Technology, Coimbatore, Kuniyamuthur, Tamil Nadu 641008 India.

- pre-processed by gaussian filter for reducing the noises and smoothen the edges.
- The Dual Attention U-Network is used to segment the liver region separately from the pre-processed CXR images.
- Finally, the segmented images are fed into SDCNN to classify the TB into tri classes such as NC, PT and MT.
- The efficiency of the suggested TOUR-STAR was evaluated using the specific metrics like f1 score, accuracy, specificity, precision and recall.

The structure of the paper is organised as follows, section-2 describes the literature survey, the proposed TOUR-STAR was explained in section-3, the performance results and their comparison analysis were provided in section-4 and section-5 encloses with conclusion and future work.

#### 2. LITERATURE SURVEY

In recent years, several researches have investigated the classification of TB with DL and machine learning (ML) methods. The section that provides a review of some current research papers.

In 2024, Nafisah, S.I. and Muhammad, G., [8] suggested an TB classification system using DL models. A CXR image has a large number of dark areas that could confuse DL models and provide no information for diagnosis. Using three publicly accessible CXR datasets, it examines how well different CNN models perform in classification. With a receiver operating distinctively of 99.9% and an average accuracy of 98.7%, one of the CNN models, EfficientNetB3, obtains the maximum accuracy of 99.1%.

In 2024, Kawuma, S., et al., [9] proposed a diagnosis and detection of TB CXR images using DL. Digital CXR radiograph images were used in the study to train and validate five models which were pre-trained Transfer Learning (TL) models and one that was built from scratch. The model divides patient clinical photos into two categories: TB and normal.

In 2024, Patel, N., et al., [10] proposed a self-supervised DL tailored for TB case screening. It is asserted that the procedure of knowledge distillation through self-supervised learning and self-training cultivates a strong association amongst attention to the lesion, which could enhance the analytical precision of the model even if lesion-specific data is not available. With a noteworthy 98.14% overall accuracy and high rates of 99.44% and 95.72% recall and precision in identifying TB patients, the network effectively captures therapeutically significant characteristics.

In 2020, Rahman, T., et al., [11] suggested a TL approach with CNN for the identification of TB from the CXR. Nine distinct the effectiveness of CNN models to differentiate between TB and typical CXR pictures was evaluated. DenseNet201 outperformed the full set of X-ray pictures in classification, with the segmented lung images achieving 98.6%, 98.57%, 98.56%, 98.56%, and 98.54% accuracy, precision, sensitivity, F1-score, and specificity.

In 2020, Munadi, K., et al., [12] proposed an DL algorithm to medical photos for TB detection in order to automate diagnosis. The ResNet and EfficientNet models, which had previously been trained for TL, were then fed the improved picture samples. We obtained classification accuracy and AUC values of 89.92% and 94.8% in a dataset of TB images.

In 2022, Showkatian, E., et al., [13] proposed TL method to classified TB and normal cases from the CXR using a TL method with deep CNNs. Additionally, a CNN-based TL approach was employed to distinguish among TB and normal patients utilizing CXR images using five different pretrained models: ResNet50, VGG16, Inceptionv3, VGG19 and Xception. Our suggested CNN architecture performed marginally better than the pre-trained models, with 87.0% accuracy, 88.0% precision, 87.0% sensitivity, 87.0% F1-score, and 87.0% AUC.

In 2021, Dasanayaka, C. and Dissanayake, M.B., et al., [14] proposed a DL pipeline comprising three distinct state-of-the-art DL architectures. It offers a CXR-based automated TB screening method that is extremely accurate. This approach would be particularly beneficial in low-income nations where access to skilled medical professionals is restricted. With a classification accuracy of 97.1%, it significantly outperforms earlier research.

Based on the above literature survey, existing techniques was developed using various DL approaches to the detection of TB. However, these methods are fails to provide the high reliability rate and the process of identifying TB need more time. To address this challenge, a novel DL-based TOUR-STAR model has been proposed for more effective identification of TB from CXR images.

### 3. PROPOSED METHODOLOGY

In this research, a novel TOUR-STAR is suggested for efficient classification of TB using CXR input images. Pad Chest dataset is used as a starting point to collect the CXR images and the gathered images are pre-processed by Gaussian filter for reducing the noises and smoothen the edges. The Dual Attention U-Network is used to segment the liver region separately from the pre-processed CXR images. The segmented images are fed into SDCNN to classify the TB into tri classes such as NC, PT and MT. The proposed TOUR-STAR is presented in Figure 1.

## 3.1 Dataset description

The training set and the parameter tuning set were created by dividing the data by patient. The data, collected retrospectively from two diagnostic centers in India, included 6,350 normal CXRs, 2,914 CXRs with active TB based on radiology reports, 3,139 CXRs with various abnormalities but negative for TB in radioscopy reports, and 1,464 CXRs with positive molecular testing for TB. Additionally, there were 60,326 CXRs with various abnormalities such fibrosis, pleural effusion, or atelectasis in the PadChest dataset, in addition to 37,716 normal CXRs.

# 3.2 Pre-processing

The collected images are pre-processed by Gaussian filter for reducing the noises and smoothen the edges. Pre-processing medical images is essential to improving the accuracy and comprehensibility of diagnostic findings. The

Gaussian filter reduces noise and smooths images while maintaining important features. In the image, each pixel is subjected to a weighted average determined by a Gaussian function.

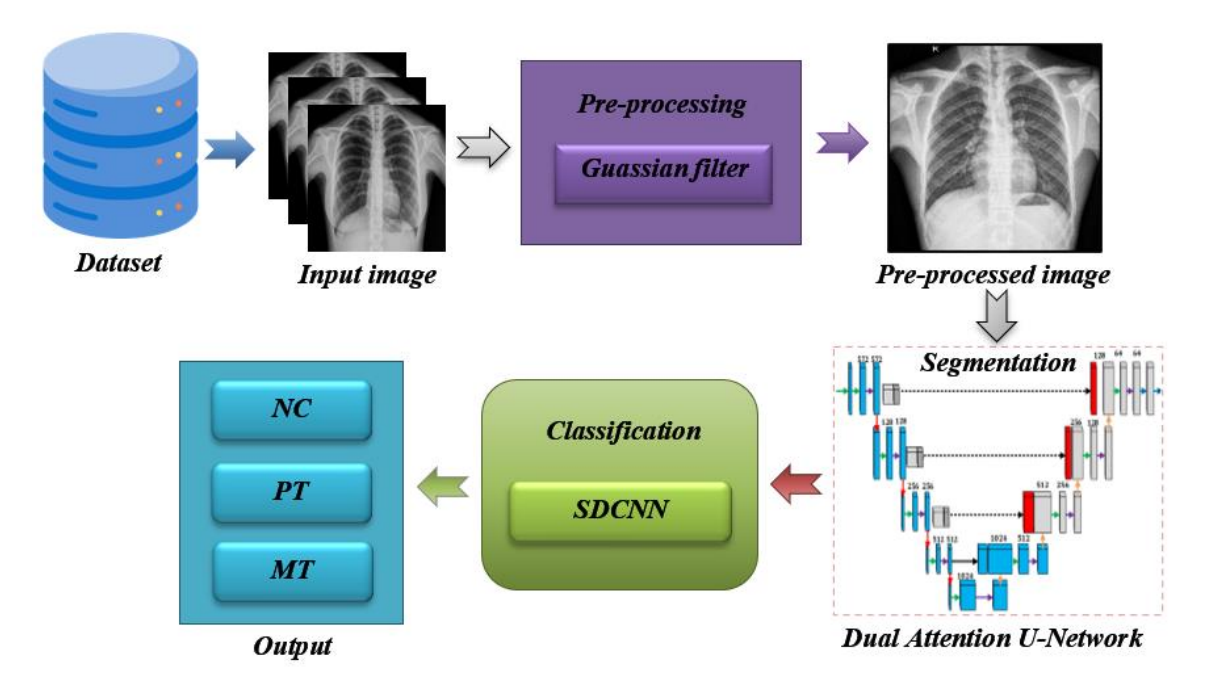


Figure 1. Proposed TOUR-STAR methodology

A Gaussian function smoothest the image by giving more weight to pixels near the center of the filter window. This gaussian function is mathematically determined as,

$$G(x,y) = \frac{1}{2\pi\sigma^2} e^{-\frac{x^2 + y^2}{2\sigma^2}}$$
 (1)

The Gaussian kernel is represented as G(x,y), the spatial coordinates of the filter are x and y, and the standard deviation of the Gaussian distribution,  $\sigma$ , determines how much smoothing is applied to the image. The following stage

produces the smoothed output image by the input image with a gaussian filter. Based on the specific requirements, the kernel size and  $\sigma$  value was changed in the properties of the input images.

# 3.3 Segmentation

The Dual Attention U-Network is used to segment the liver region separately from the pre-processed CXR images. The symmetric network consists of an encoder and a decoder.

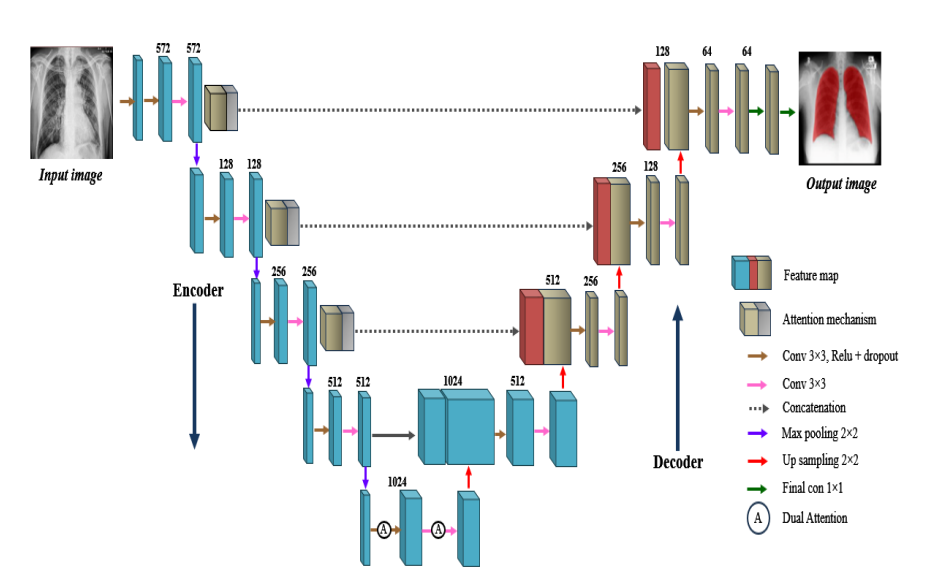


Figure 2. The Dual Attention U-Network architecture

To extract spatial data from images, the encoder uses a convolutional network's standard architecture. This convolution module consists of two 3x3 convolutions, a max-pooling operation with a 2x2 pooling size, and two strides. The number of filters in the convolution doubles every time this block is iterated. Both encoder and decoder are connected with two 3x3 convolutions. The encoder and decoder features are used to construct the segmentation map. By transposing the feature map 2 x 2, the decoder divides the feature channels in half and up samples the feature map at the same time. Two 3 × 3 convolution processes are then carried out once more. The encoder repeats this series of two convolution operations and up sampling four times, splitting the number of filters at each iteration. To create the final segmentation map, a  $1 \times 1$  convolution method is ultimately used. Every U-Net convolutional layer except the last uses the rectified linear unit as the activation function. The U-Net architecture also adds a skip connection between the decoder and encoder. In order to propagate the concatenated feature maps to the subsequent layers, they are connected with the output of the up-sampling process. The network can retrieve spatial information lost during pooling due to the skip connections. Figure 2 shows the Dual Attention U-Network architecture.

Dual Attention U-Network can be formulated as:

$$Y = A_s(f(X)) \odot A_c(f(X)) \tag{2}$$

Where, X be the input image, f(X) be the U net architecture applied to the input,  $A_s(X)$  represents the spatial attention map,  $A_c(X)$  denotes the channel attention map, f(X) is the Dual Attention U-Network feature extraction,  $A_s(f(X))$  is the spatial attention applied to the U net feature map,  $A_c(f(X))$  is the channel attention applied to the Dual Attention U-Network feature map and  $\odot$  represents the element-wise multiplication.

# 3.4 Classification

SDCNN to classify the classes of TB as normal controls Pulmonary Tuberculosis (PT) and Tuberculosis (MT). The development of artificial neural networks (ANNs) was motivated by the principles observed in the biological nervous system. Instead of using the rate or level encodings that were employed in previous neural models, biological neurons appear to do computation in the temporal domain. These biological insights have led to the development of spiking neural networks (SNNs). In essence, SNNs are networks of neurons with spikes. In CNN, real values  $(x_{i,j}, \text{ and } y_i)$  are transferred across layers, but in SNN binary spikes  $b_{i,j}^t$  and  $y_i^t$  are used. Therefore, to construct the weighted sum, masked summation is utilized. The membrane voltage is increased by the weighted total at each time step,  $V_i$  the neuron generates 1 and  $V_i$  falls by  $\theta_i$  when  $V_i$ decreases by  $\theta_i$ . When  $V_i$  exceeds a predetermined threshold. Otherwise, it generates 0.

$$\alpha_{i}^{t} = \sum_{i=0}^{n} (w_{i,i}^{t}.b_{i,i}^{t})$$
(3)

$$V_i^t = V_i^{t-1} + \alpha_i^t; \tag{4}$$

$$Y_i^t = \begin{cases} 1, & V_i^t > \theta_i \\ 0, & \text{otherwise} \end{cases}$$
 (5)

$$\begin{cases} V_i^t - \theta_{i,} & V_i^t > \theta_{i,} \\ V_i^t, & otherwise \end{cases};$$
 (6)

Every neuron is subjected to the integrate fire (IF) model in this work. The variable  $V_i^t$  is computed to store prior data during the integration stage.  $V_i^{t-1} + \sum_{j=0}^{n} (w'_{j=0}, X_l) t$  represents the time step.

This method creates spaces between the next component and the previous piece, therefore expanding the kernel (input). In short, pixel skipping is added to convolution to cover a larger area of the input. In order to get a larger receptive field without introducing more parameters, CNN employ dilated convolution, also known as aurous convolution. The architecture of a SDCNN is displayed in Figure 6. Because CNN employs additions rather than multiplications for inputs and weights, SNN spends a significant amount of energy less than dilated CNN.

## 4. RESULTS AND DISCUSSION

This section uses Matlab-2019b to assess the proposed model efficiency, a DL toolbox. The TOUR-STAR is estimated using several measures such as specificity, accuracy, precision, recall and sensitivity. Benchmarks include TOUR-STAR method overall accuracy rates, performance explicitly stated and evaluated. The visualization outcomes of the proposed method classification using the Pad Chest dataset are shown in Figure 3.

| Input image  | Pre-processing   | Segmentation | Classification |
|--------------|--|--------------|----------------|
|              |  |              | NC             |
| SHEET, STORY | STATE OF THE PARTY |              | PT             |
|              |  |              | МТ             |

**Figure 3.** Experimental result of the proposed TOUR-STAR

Figure 3 illustrates the simulation result of the proposed TOUR-STAR with the different input image samples. The input images (column 1) from the Pad Chest dataset are preprocessed using Gaussian filter as displayed in column 2. The segmented results are shown in column 3 and the column 4 displayed the classification results such as NC, PT and MT.

### 4.1 Performance analysis

A proposed TOUR-STAR model was assessed based on f1 score, specificity, recall, accuracy and precision.

$$Specificity = \frac{T_{neg}}{T_{neg} + F_{pos}} \tag{7}$$

$$Precision = \frac{T_{pos}}{T_{pos} + F_{pos}}$$
 (8)

$$Recall = \frac{T_{pos}}{T_{pos} + F_{neg}} \tag{9}$$

$$Accuracy = \frac{T_{pos} + T_{neg}}{Total\ no.of\ samples}$$
 (10)

$$F1\ score = 2\left(\frac{Precision + Recall}{Precision + Recall}\right) \tag{11}$$

Where  $T_{neg}$  and  $T_{pos}$  specifies true negatives and true positives of the sample images,  $F_{neg}$  and  $F_{pos}$  specifies false negatives and false positives of the sample images.

**Table 1.** Performance assessment of the proposed TOUR-STAR model

| Classe | Accurac | Specificit | Precisio | Recal | F1   |
|--------|---------|------------|----------|-------|------|
| S      | у       | у          | n        | 1     | scor |
|        |         |            |          |       | e    |
| NC     | 99.38   | 97.45      | 97.23    | 90.67 | 89.6 |
| INC    | 99.30   | 97.43      | 91.23    | 90.07 | 8    |
|        |         |            |          |       | 0    |
| PT     | 98.76   | 96.23      | 96.67    | 95.79 | 91.9 |
|        |         |            |          |       | 7    |
|        |         |            |          |       |      |
| MT     | 98.57   | 98.79      | 94.46    | 93.61 | 94.6 |
|        |         |            |          |       | 8    |
|        |         |            |          |       |      |

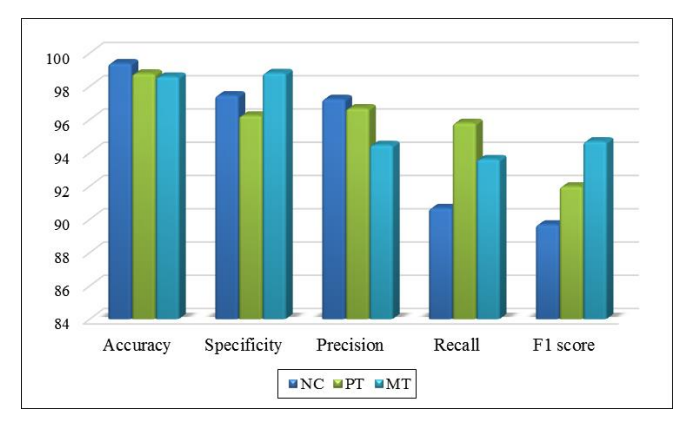


Figure 4. Graphical representation of performance analysis

Table 1 displays the classification performance obtained by proposed TOUR-STAR model for classifying the TB. F1 score, recall, precision, accuracy and specificity, are metrics that determine the performance. A total accuracy of 98.90% is achieved by the proposed TOUR-STAR model using the dataset. The proposed TOUR-STAR model also achieves 96.12%, 92.11%, 97.49% and 93.35% overall precision, f1 score, specificity and recall. Figure 4 provides a graphic representation of the TOUR-STAR model performance assessment.

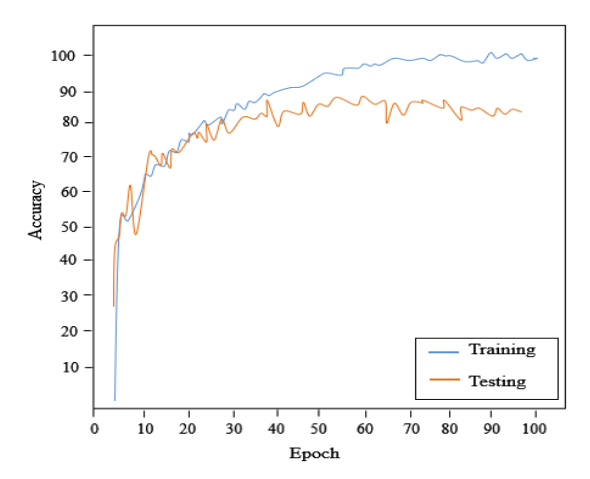


Figure 5. Training and testing accuracy curve of SDCNN

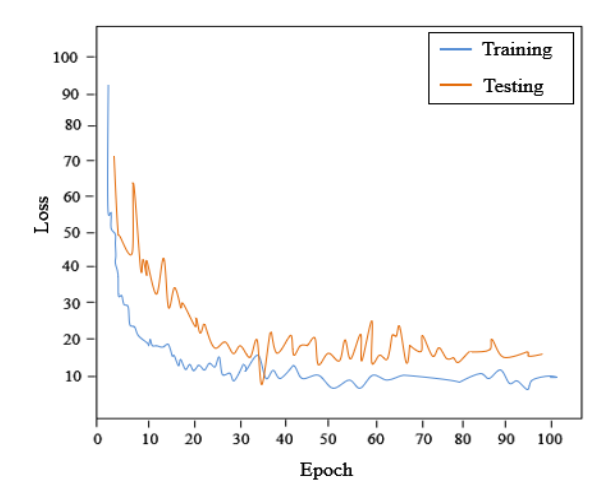


Figure 6. Training and testing loss curve of SDCNN

Figure 5 shows epochs on the x and y axes, along with a comparison of testing and training accuracy. Figure 6 indicates a loss curve plotted against epochs, which shows that the loss decreases with rising epochs. The proposed procedure yields an accurate result with a reasonably low loss of 1.1%. The proposed TOUR-STAR achieved 98.90% training and testing accuracy based on the number of epochs, with a low percentage of errors.

### 4.2 Comparative analysis

The effectiveness of DL network was determined in order to validate that the TOUR-STAR generates results with a high level of accuracy. The suggested SDCNN and four classifiers, ResNet, AlexNet, RegNet and GoogleNet were compared. A variety of measures were used to evaluate each DL techniques performance including accuracy, recall, fl score, precision and specificity.

**Table 2.** Comparison between DL networks and proposed TOUR-STAR

| Network | Accura | Specifici | Precisi | Reca | F1   |
|---------|--------|-----------|---------|------|------|
| s       | cy     | ty        | on      | 11   | scor |
| ResNet  | 93.65  | 90.04     | 94.23   | 92.2 | 90.2 |

| AlexNet       | 97.28 | 94.58 | 91.04 | 95.0<br>5 | 91.4      |
|---------------|-------|-------|-------|-----------|-----------|
| RegNet        | 94.45 | 96.24 | 92.45 | 94.2<br>8 | 94.2<br>4 |
| GoogleN<br>et | 98.07 | 92.56 | 95.27 | 90.7<br>5 | 93.7      |
| SDCNN         | 98.90 | 97.49 | 96.12 | 93.3<br>5 | 92.1<br>1 |

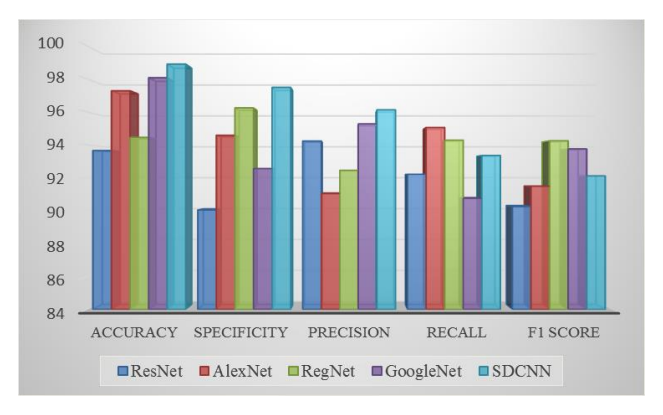


**Figure 7.** Comparison of existing DL network with SDCNN

To compare several DL networks based on performance measures and determine an appropriate percentage of classification accuracy, Table 2 was examined. The proposed SDCNN outperforms ResNet, AlexNet, RegNet, and GoogleNet by 5.30%, 1.63%, 4.49% and 0.83% in terms of overall accuracy range. Figure 7 shows a graphic representation of the SDCNN comparative evaluation.

**Table 3.** Comparison of existing method versus proposed TOUR-STAR

| Authors                                       | Methods      | Accuracy |
|---|--------------|----------|
| Nafisah, S.I. and<br>Muhammad, G., (2024) [8] | CNN          | 98.7%    |
| Patel, N., et al., (2024) [10]                | DNN          | 98.14    |
| Munadi, K., et al., (2020)<br>[12]            | EfficientNet | 94.8%    |
| Proposed                                      | SDCNN        | 98.90%   |

Table 3 demonstrates the assessment among the existing methods and the suggested method. The suggested TOUR-STAR model achieves the overall accuracy by 0.20%, 0.76% and 4.14% comparing to the existing method such as CNN, DNN and EfficientNet. However, the proposed TOUR-STAR model produced better fallouts than the previous methods. As a result, the proposed model's attains high prediction rate for classifying the TB.

#### 5. CONCLUSION

In this research, a novel DL-based TOUR-STAR model was proposed for classifying the TB into tri classes. Pad Chest dataset is used as a starting point to collect the CXR images and the gathered images are pre-processed by Gaussian filter for reducing the noises and smoothen the edges. The Dual Attention U-Network is used to segment the liver region separately from the pre-processed CXR images. Finally, the segmented images are fed into SDCNN to classify the TB into tri classes such as NC, PT and MT. The proposed TOUR-STAR is evaluated based on its specificity, fl score, precision, recall and accuracy. The proposed SDCNN outperforms ResNet, AlexNet, RegNet, and GoogleNet by 5.30%, 1.63%, 4.49% and 0.83% in terms of overall accuracy range. The suggested TOUR-STAR model achieves the overall accuracy by 0.20%, 0.76% and 4.14% comparing to the existing method such as CNN, DNN and EfficientNet. In the future, the proposed model can be enhanced by incorporating transfer learning techniques to improve its adaptability for detecting neurodegenerative diseases beyond TB. This enhancement with TL allows the model to control pre-trained knowledge for reducing the training time in the accurate classification of different TB diseases.

#### CONFLICTS OF INTEREST

The authors declare that they have no known competing financial interests or personal relationships that could have appeared to influence the work reported in this paper.

#### FUNDING STATEMENT

Not applicable.

## **ACKNOWLEDGEMENTS**

The author would like to express his heartfelt gratitude to the supervisor for his guidance and unwavering support during this research for his guidance and support.

## REFERENCES

- [1] E. Kotei, and R. Thirunavukarasu, "A comprehensive review on advancement in deep learning techniques for automatic detection of tuberculosis from chest X-ray images", *Archives of Computational Methods in Engineering*, vol. 31, no. 1, pp. 455-474, 2024. [CrossRef] [Google Scholar] [Publisher Link]
- [2] M. Oloko-Oba, and S. Viriri, "A systematic review of deep learning techniques for tuberculosis detection from chest radiograph", *Frontiers in medicine*, vol. 9, pp. 830515, 2022. [CrossRef] [Google Scholar] [Publisher Link]
- [3] S.M. Fati, E.M. Senan, and N. ElHakim, "Deep and hybrid learning technique for early detection of tuberculosis based on X-ray images using feature fusion", *Applied Sciences*, vol. 12, no. 14, pp.7092, 2022. [CrossRef] [Google Scholar] [Publisher Link]
- [4] S.M. Fati, E.M. Senan, and N. ElHakim, "Deep and hybrid learning technique for early detection of tuberculosis based on X-ray images using feature fusion", *Applied Sciences*, vol. 12, no. 14, pp.7092, 2022. [CrossRef] [Google Scholar] [Publisher Link]
- [5] O. Faruk, E. Ahmed, S. Ahmed, A. Tabassum, T. Tazin, S. Bourouis, and M. Monirujjaman Khan, "[Retracted] A Novel and Robust Approach to Detect Tuberculosis Using Transfer Learning", *Journal of healthcare engineering*, vol. 2021, no.

- 1, pp.1002799, 2021. [CrossRef] [Google Scholar] [Publisher Link]
- [6] C.J. Hou, L.P. Jack, A. Baharum, and N.A.M. Noor, "Enhancement of tuberculosis detection using ensemble classifier with quadtree method: A preliminary study", *Journal* of Modern Mechanical Engineering and Technology, vol. 7, pp.1-6, 2020. [CrossRef] [Google Scholar] [Publisher Link]
- [7] V. Sharma, S.K. Gupta, and K.K. Shukla, "Deep learning models for tuberculosis detection and infected region visualization in chest X-ray images", *Intelligent Medicine*, vol. 4, no. 2, pp. 104-113, 2024. [CrossRef] [Google Scholar] [Publisher Link]
- [8] S.I. Nafisah, and G. Muhammad, "Tuberculosis detection in chest radiograph using convolutional neural network architecture and explainable artificial intelligence", *Neural Computing and Applications*, vol. 36, no. 1, pp.111-131, 2024. [CrossRef] [Google Scholar] [Publisher Link]
- [9] S. Kawuma, E. Kumbakumba, V. Mabirizi, D. Nanjebe, K. Mworozi, A. Oyesigye Mukama, and L. Kyasimire, "Diagnosis and Classification of Tuberculosis Chest X-ray Images of Children Less Than 15 years at Mbarara Regional Referral Hospital Using Deep Learning", *Journal of AI and Data Mining*, vol. 12, no. 2, pp. 315-324, 2024. [CrossRef] [Google Scholar] [Publisher Link]
- [10] N. Patel, A. Wong, and A. Ebadi, "Empowering Tuberculosis Screening with Explainable Self-Supervised Deep Neural Networks", arXiv preprint arXiv:2406.13750. 2024. [CrossRef] [Google Scholar] [Publisher Link]
- [11] T. Rahman, A. Khandakar, M.A. Kadir, K.R. Islam, K.F. Islam, R. Mazhar, T. Hamid, M.T. Islam, S. Kashem, Z.B. Mahbub, and M.A. Ayari, "Reliable tuberculosis detection using chest X-ray with deep learning, segmentation and visualization", *Ieee Access*, vol. 8, pp. 191586-191601, 2020. [CrossRef] [Google Scholar] [Publisher Link]
- [12] K. Munadi, K. Muchtar, N. Maulina, and B. Pradhan, "Image enhancement for tuberculosis detection using deep learning", *IEEE Access*, vol. 8, pp. 217897-217907, 2020. [CrossRef] [Google Scholar] [Publisher Link]
- [13] E. Showkatian, M. Salehi, H. Ghaffari, R. Reiazi, and N. Sadighi, "Deep learning-based automatic detection of tuberculosis disease in chest X-ray images", *Polish journal of radiology*, vol. 87, pp.e118, 2022. [CrossRef] [Google Scholar] [Publisher Link]

- [14] C. Dasanayaka, and M.B. Dissanayake, "Deep learning methods for screening pulmonary tuberculosis using chest X-rays", Computer Methods in Biomechanics and Biomedical Engineering: Imaging & Visualization, vol. 9, no. 1, pp. 39-49, 2021. [CrossRef] [Google Scholar] [Publisher Link]
- [15] K. Okada, N. Yamada, K. Takayanagi, Y. Hiasa, Y. Kitamura, Y. Hoshino, S. Hirao, T. Yoshiyama, I. Onozaki, and S. Kato, "Applicability of artificial intelligence-based computer-aided detection (AI–CAD) for pulmonary tuberculosis to community-based active case finding", *Tropical Medicine and Health*, vol. 52, no. 1, pp.2, 2024. [CrossRef] [Google Scholar] [Publisher Link]

#### **AUTHORS**



**R. Shobana,** Assistant Professor, Department of Computer Science and Engineering, S.A. Engineering college, Chennai, Thiruverkadu, Tamil Nadu 600077 India



Abitha VK Lija completed her B.E in CSE from CSI Institute of Technology, Thovalai affilated to Anna University. She completed her M.E in CSE from Jerusalem College of Engineering affiliated to Anna University. She is currently working as Assistant Professor in the Department of CSE in Meenakshi College of Engineering, Chennai, India. She is currently pursuing Ph.D. in the Department of

Computer Science and Engineering in S.A. Engineering College under Anna University, Chennai, India. Her area of interest includes IoT, Cyber security, big data, Deep learning and Machine Learning.



S. Shikky Marice Research Scholar with more than 4 years of teaching experience. I obtained my M.E in Communication Systems Engineering from Cape Institute of Technology (affiliated to Anna University) in the year 2013. My research interests lie in the domain of Computer Vision, Pattern Recognition, Anomaly Detection & Clustering.

Arrived: 16.11.2023 Accepted: 18.12.2023